ROBUST CONTROL DESIGN FOR THE ELEVATION AXIS STABILIZATION OF THE M256E1 LONG GUN

V. R. Marcopoli, M. S. Ng, and C. R. Wells

General Dynamics Land Systems, 38500 Mound Road, Sterling Heights, MI 48312

A key feature of the Abrams tank is the ability to deliver precision fire during on-the-move vehicle operation. The increased flexibility of a longer gun tube presents a significant additional challenge to stabilization system design. To address the increased difficulties of this problem, an approach to gun stabilization is presented that uses modern robust control techniques to achieve muzzle-pointing accuracy. Such control design methods are model-based, and thus require an accurate mathematical description of the system dynamics. Following a brief description of the model used, the control objectives of performance and robustness are cast in a general framework that precisely quantifies these design goals as optimization objectives. The method of μ-synthesis is then applied, yielding a controller that realizes the objectives. The effectiveness of this control design is illustrated via its implementation in the M256E1 Long Gun demonstration vehicle. Test results of the new controller are compared with a "classically" tuned controller.

1 INTRODUCTION

In order to address future needs for improving the lethality of the M1A2 main battle tank, the army has funded a demonstration program to integrate a longer gun tube. The long tube is based on the German L55 tube, made by Rheinmetall, and is 4.3 feet (1.3 m) longer than the conventional M256 120 mm gun tube. Unfortunately, with the increased length comes increased flexibility, which, if not addressed properly, can introduce significant accuracy degradation when firing on the move.

It is the job of the stabilization system to maintain proper aiming of the gun when the vehicle is moving. In order to address the increased demands made on the stabilization system due to the longer gun tube, a new approach to stabilization design has been investigated. The method is from the area of robust control, called μ-synthesis, and requires an accurate model of the system dynamics. The goal is to use the system dynamics to derive a *design* model that allows control design objectives to be quantified via its inputs and outputs. Once this is accomplished, the μ-synthesis optimization framework can be directly applied to obtain a controller that achieves the design goals. In order to mitigate risk and facilitate evaluation of the new method, a classical stabilization scheme has also been developed. The two approaches are compared in Section 5.3.

The primary goal of this paper is to introduce the general design concepts and summarize how they are applied to the gun stabilization problem. Due to space limitations and program sensitivity, information regarding the modeling details, as well as specific quantitative system properties and performance numbers have been omitted.

2 ELEVATION DYNAMICS

The elevation model framework is shown schematically in Figure 1.

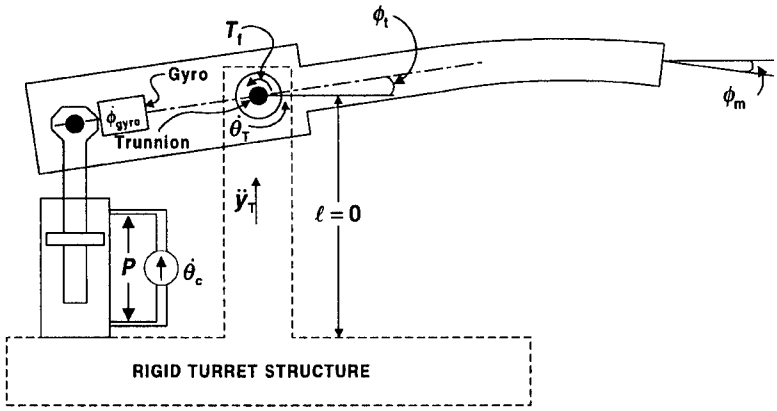

FIGURE 1: ELEVATION SYSTEM MODELING SCENARIO

The "input" quantities are:

T_f = Trunnion friction torque (in-lb)

$\dot{\theta}_T$ = Rotational turret motion (rad/sec)

$\ddot{y}_T$ = Translational turret motion (in/sec^2)

$\dot{\theta}_c$ = Gun rate command (rad/sec)

and the "output" quantities are:

ϕ_m = Muzzle angle (rad)

ϕ_t = Trunnion angle (rad)

$\dot{\phi}_{gyro}$ = Gyro angular rate (rad/sec)

P = Hydraulic pressure (psi)

The gun tube model assumes small angles and point masses. Flexibility is introduced by constraining the motion of the point masses via three bending modes, which are obtained from mass and stiffness distributions, using "pin" constraints at the trunnion and actuator connection points. This yields an 8th order gun tube model. The hydraulic actuator is driven by a flow command, which is equivalent to the gun angular rate command, $\dot{\theta}_c$, that opens a valve to port oil from one side of the piston to the other. Hydraulic leakage and first order oil compressibility dynamics are also accounted for in the actuator model. A pressure difference across the piston is thus generated, resulting in a force applied to accelerate the gun. To account for the unbalance of the longer tube, the elevation mechanism is equilibrated. This is modeled as a simple pressure source that sums with the actuator output to provide the total actuator force on gun. Nonlinear effects considered in the model are trunnion friction and hydraulic loading. This modeling

scenario is described more precisely via the block diagram shown in Figure 2. Detailed development of this model is given in [1]

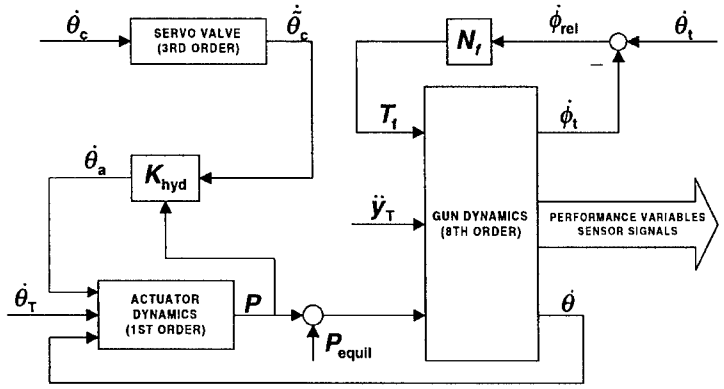

FIGURE 2: BLOCK DIAGRAM MODEL OF ELEVATION SYSTEM

The time varying gain, K_{hyd}, is defined via

$$K_{hyd} = \begin{cases} \sqrt{1-\min\{1,|P/P_S|\}}, & \dot{\theta}_{cmd} P \geq 0 \\ \sqrt{1+|P/P_S|}, & \dot{\theta}_{cmd} P < 0 \end{cases}$$

and models hydraulic loading effects (P_S is the supply pressure). For reasons that are described in Section 3.3, it is convenient to rewrite the hydraulic nonlinearity as an actuator perturbation. The equivalence is shown in Figure 3, where $\delta_{act} = K_{hyd} - 1$, and the perturbation input and output are defined as q_{act} and p_{act}, respectively.

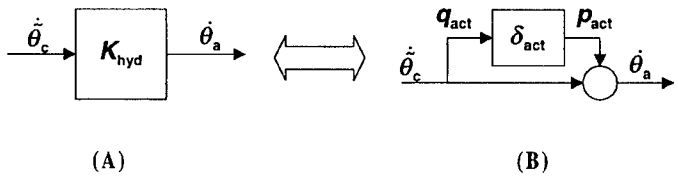

FIGURE 3: (A) HYDRAULIC NONLINEARITY (B) EQUIVALENT PERTURBATION FORM

The nonlinearity N_f is a simple trunnion bearing coulomb-type friction model, defined as

$$N_f = T_{f,max} \frac{2}{\pi} \tan^{-1} S\dot{\phi}_{rel}$$

where $T_{f,max}$ is the friction magnitude, and S is a "shaping" parameter for adjusting the sharpness of the transition of the friction nonlinearity about zero relative velocity. Combining Figure 2 and Figure 3, the gun system interconnection is redrawn in simpler form in Figure 4, providing a concise input-output view of the plant.

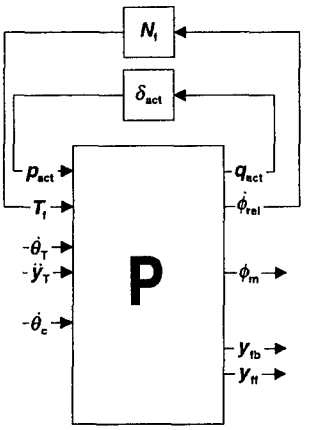

FIGURE 4: ALTERNATIVE BLOCK DIAGRAM VIEW OF ELEVATION SYSTEM (OPEN LOOP)

The vector variables y_{fb} and y_{ff} are introduced to represent the feedback and feedforward sensor signals, respectively, which are sent to the controller. The feedback vector is defined as:

$$y_{fb} = \begin{bmatrix} H_{rslvr}\phi_t \\ H_{gyro}\dot{\phi}_{gyro} \\ H_{AA}P \end{bmatrix} \tag{1}$$

where the variables $H_{()}$ denote relevant filtering dynamics applied to the respective physical quantities. In the case of the trunnion and gyro feedback signals, the sensor dynamic is used, whereas for the pressure feedback, the software anti-alias filter is used because this dynamic dominates the sensor dynamic. The feedforward vector for the long gun system is:

$$y_{ff} = \begin{bmatrix} H_{gyro}\dot{\theta}_T \\ H_{AA}\ddot{y}_T \end{bmatrix} \tag{2}$$

The use of an accelerometer feedforward sensor has been shown to be advantageous when stabilizing out-of-balance armaments [2].

It is important to note that the nominal gun plant, P, is a *linear* system. The nonlinearities are shown explicitly, and enter the system as perturbations. This input-output view of the gun system shown in Figure 4 is a very convenient means of depicting this system, since it puts primary focus on the fundamental linear system behavior while maintaining nonlinear fidelity. More importantly, this framework facilitates the use of modern robust control methodologies, where a linear controller is designed to meet objectives that include nonlinear effects. This is the subject of the next section.

3 ROBUST CONTROL FRAMEWORK

The formulation of a control design problem using tools from robust control theory requires the system to be put into a standard framework. To this end, consider Figure 5, which

depicts the nominal linear plant system, P (from Figure 4), connected to the controller, K, and perturbations δ_{act} and Δ_{fb}.

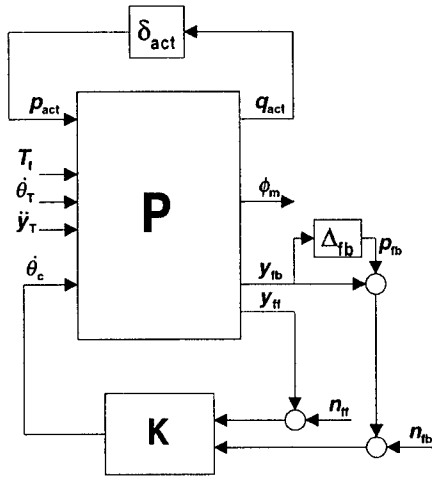

FIGURE 5: CLOSED LOOP SYSTEM

Note the trunnion friction, T_f, is now viewed as an external disturbance, along with the terrain inputs, $\dot{\theta}_T$ and $\ddot{y}_T$. The nonlinear feedback that generates T_f (see Figure 4) is thus neglected. This simplification has proven to be a reasonable assumption, since the trunnion friction is typically small and its effect is primarily in increased errors, and not in any more complicated nonlinear phenomenon such as limit cycling or instability. Finally, the feedback connection is augmented with measurement noise input vectors, n_{fb} and n_{ff}, and a diagonal matrix perturbation, Δ_{fb}. These modifications are necessary when using optimization-based techniques for control design, so the resulting controller is not overly sensitive to measurement noise, and robust to nonlinearities and modeling errors; details are given in the remaining development.

The first step in formulating a robust control design is to group the signals of Figure 5 into three sets of vector input/output signals: 1) Controller variables, u and y, 2) Performance variables, z and w, and 3) Robustness variables, p and q. These standard signals can be defined for any control problem; the task of the design engineer is to choose them wisely so that a meaningful controller optimization problem can be formulated. Once these signal sets are defined, the Figure 5 can be redrawn in the standard robust control block diagram shown in Figure 6(A), where the controller, K, and combined perturbation matrix, Δ, defined in Figure 6 (B), are connected to the so-called "design plant," P_d [3].

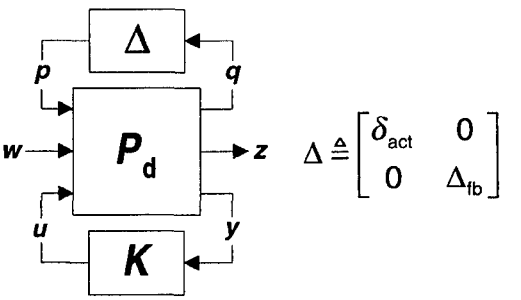

FIGURE 6: (A) STANDARD ROBUST CONTROL BLOCK DIAGRAM (B) DEFINITION OF Δ

Descriptions of the three signal sets are now given, along with the choices made for the current gun stabilization problem. Following these definitions, the robust control design goals will be formulated in terms of this standard framework.

3.1 Control Variables

The control variables, u and y, represent the actuator input and sensor output signals, respectively, and define how the controller, K, connects to the system. In the M1A2 system, u is simply the gun rate command, $\dot{\theta}_c$. The sensor vector, y, consists of all signals available to the controller, and is defined as follows:

$$y = \begin{bmatrix} y_{fb} + n_{fb} + p_{fb} \\ y_{ff} + n_{ff} \end{bmatrix}$$

where y_{fb} and y_{ff} are from (1) and (2), respectively, and n_{fb}, n_{ff}, and p_{fb} are from Figure 5.

3.2 Performance Variables

The performance variables, w and z, represent, respectively, the external system disturbances, and the signals which are required to remain small in the presence of such disturbances. The input vector, w, is a vector of all modeled external influences on the plant. Typical elements of this vector include disturbances, noise, and reference commands. This can be thought of as a vector of "generalized" disturbances, and is often referred to in the literature as the *exogenous inputs* [3]. The performance output vector, z, often called the *regulated variables,* is defined such that all control system performance objectives are captured, where each component in z is chosen such that "smaller is better." For the current stabilization design framework, these variables are chosen as follows:

$$w \triangleq \begin{bmatrix} d \\ \hline n \end{bmatrix} = \begin{bmatrix} T_f \\ \dot{\theta}_T \\ \ddot{y}_T \\ \hline n_{fb} \\ n_{ff} \end{bmatrix}, \quad z \triangleq \begin{bmatrix} e \\ u \end{bmatrix} = \begin{bmatrix} \phi_m \\ \dot{\theta}_c \end{bmatrix} \tag{3}$$

where the notation $\triangleq$ is used to denote a redefinition of the performance variables in a more detailed form. Specifically, the w vector is generically partitioned into *disturbance* and *noise* (vector) components. The reason for such a distinction is primarily in the frequency content of such signals. Disturbances occur typically in lower, operational frequency ranges, whereas noise signals typically have higher frequency content. For the current system, the friction and terrain components are natural choices for the disturbance vector d. The two sensor noise components are grouped into the noise vector, n. The z vector is generally made up of an error component, e, and an actuator command component, u. This reflects the practical control design principle that performance be achieved (e.g. small "errors") without excessive actuator effort, due to physical system limitations. For the current problem of muzzle stabilization, e is simply defined as the muzzle angle, and u is the gun rate command, $\dot{\theta}_c$.

3.3 Robustness Variables

When applying optimization-based design algorithms, it is critical to include robustness considerations to account for system perturbations and modeling errors. The robustness variables can be thought of as a way to introduce conservatism in the design by preventing over-optimization that would occur by assuming that the model is perfect. Alternatively stated from a classical control design viewpoint, designing for robustness is a way to design in stability margins. The goal of this section is simply to establish the "hooks" in the design framework that will later be used to provide for design robustness. The specific manner in which these variables are used to address robustness issues is described in Section 4.2

As alluded to in Figure 5 and the accompanying discussion, robustness issues are addressed by inserting perturbations into the linear closed loop system, in order to account for discrepancies between the linear model and the true physical plant. Recall multiplicative perturbations are inserted into the actuator path via δ_{act} and each sensor path via Δ_{fb}. The combined perturbation matrix, Δ, is thus a 4×4 diagonal matrix containing the individual perturbations. For notational simplicity, the perturbations will be denoted as $\delta_i, i=1\ldots4$, where $\delta_1 = \delta_{act}$ and δ_2, δ_3, and δ_4 represent the sensor perturbations in the position, feedback gyro, and pressure channels. Furthermore, these perturbations are *complex-valued*, and thus account for model discrepancies in both magnitude and phase. Finally, in the remaining development, the perturbations are normalized to unit magnitude, with their sizes specified explicitly via weighting parameters, w_{q_i}. The structure of the individual perturbations is shown in Figure 7.

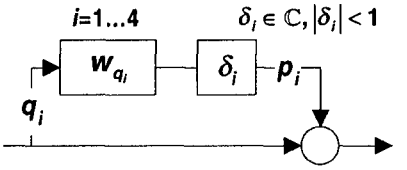

FIGURE 7: MULTIPLICATIVE PERTURBATIONS

It should be noted here that the w_{q_i} parameters can be frequency dependent; this is useful since model uncertainty is typically small at low frequencies and increases in size at high frequencies. Using the notation of Figure 5, this perturbation framework gives rise to the following assignments for the general robustness variables p and q:

$$p = \begin{bmatrix} p_{\text{act}} \\ p_{\text{fb}} \end{bmatrix}, \quad q = \begin{bmatrix} q_{\text{act}} \\ y_{\text{fb}} \end{bmatrix}$$

4 ROBUST CONTROL DESIGN SPECIFICATION

The manner in which the above framework is used to specify control design objectives is now described. The goal of the design is to achieve *robust performance*. Such a design involves optimization criteria that address performance and robustness issues. The method in which performance is specified is described in Section 4.1; Section 4.2 describes the robustness framework. Finally, Section 4.3 describes how both design goals are combined into a single design specification via the concept of μ. See [4] for more details on the concepts presented here.

4.1 The H_∞ Performance Criterion

Using the signals defined in Section 3, performance can be concisely quantified via the linear relationship shown in Figure 6 from w to z, denoted H_{zw}. Since z and w are vectors, H_{zw} is a transfer matrix. Note that this relationship is a function of the controller, K. Therefore, K can be thought of as the optimization variable that must be chosen to make H_{zw} "desirable," in some sense.

The precise specification of performance with H_{zw} requires the performance inputs and outputs to be normalized. This is necessary in order to capture order of magnitude in the vector components that exist because of 1) unit differences, 2) typical sizes of the exogenous inputs, and 3) relative importance, or penalties, of the regulated variables, normalized such that zero represents no importance and 1 represents maximum importance. When considering issue 3) it is typical to frequency weight these penalties, because in practical control problems, performance objectives are often emphasized differently at different frequencies. A typical example is that goals such as disturbance rejection and reference tracking are important at low frequencies, whereas noise rejection and robustness to modeling errors are more important at high frequencies (the latter is due to the fact that models eventually break down at high frequencies).

The above described normalization is accomplished by cascading input and output weightings, W_w and W_z, to the standard block diagram, shown in Figure 8, where it also shows, via dotted lines, the focus of performance specification in the general framework (i.e. p and q are not considered).

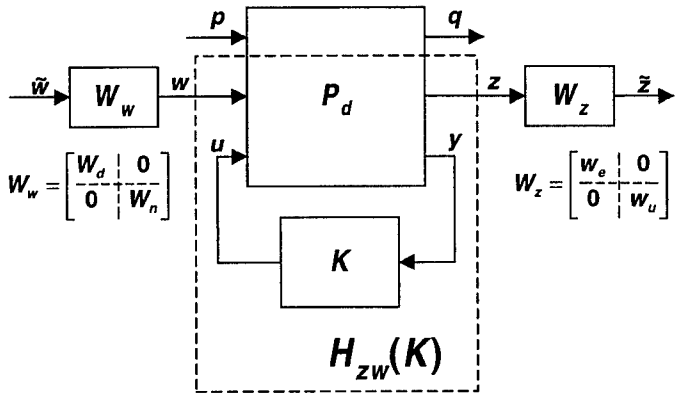

FIGURE 8: PERFORMANCE SPECIFICATION FRAMEWORK

Observe that W_w and W_z are partitioned according to the structure of the input and output performance vectors given in (3). Also, the weighting matrices have a diagonal structure, which has the effect of multiplying the i^{th} component of its input by the $(i,i)^{\text{th}}$ element of the weight matrix, as follows:

$$W_w = \left[\begin{array}{c|c} W_d & 0 \\ \hline 0 & W_n \end{array}\right] = \left[\begin{array}{ccc|cc} w_{T_f} & 0 & 0 & & \\ 0 & w_{\dot{\theta}_T} & 0 & 0 & \\ 0 & 0 & w_{\ddot{y}_T} & & \\ \hline & & & w_{n_{fb}} & 0 \\ & 0 & & 0 & w_{n_{ff}} \end{array}\right], \quad W_z = \left[\begin{array}{c|c} w_e & 0 \\ \hline 0 & w_u \end{array}\right] \tag{4}$$

The method used to choose these parameters is described in the Section 5.1. The transfer matrix providing the desired performance specification can now be written, relating the normalized exogenous input vector, $\tilde{w}$, to the normalized regulated variable vector, $\tilde{z}$:

$$H_{\tilde{z}\tilde{w}} = W_z H_{zw} W_w \tag{5}$$

Since (5) describes a generalized disturbance rejection problem (i.e. smaller is better), a mathematical concept of the "size" of this transfer matrix is needed which will precisely quantify the level of disturbance rejection. To this end, consider the *maximum singular value* of the (complex-valued) matrix $H_{\tilde{z}\tilde{w}}(j\omega)$, denoted $\bar{\sigma}\left(H_{\tilde{z}\tilde{w}}(j\omega)\right)$, defined as:

$$\bar{\sigma}\left(H_{\tilde{z}\tilde{w}}(j\omega)\right) = \max_{\omega \neq 0} \frac{\left\| H_{\tilde{z}\tilde{w}}(j\omega)\tilde{w} \right\|}{\left\| \tilde{w} \right\|}$$

where $\tilde{w}$ is a complex-valued vector, and $\|x\| = x^* x$ is the standard Euclidean norm measure for a complex vector, x. Note for the scalar case, $\bar{\sigma}(h(j\omega)) = |h(j\omega)|$. The maximum singular value can be interpreted as characterizing the maximum amplification of sinusoidal input vectors, as a function of frequency, and is a generalization of the scalar concept of the frequency response of a transfer function. Given this frequency response concept for $H_{\tilde{z}\tilde{w}}$, the desired measure of its size is given by the ∞-*norm*, defined as:

$$\|H_{\tilde{z}\tilde{w}}\|_\infty = \max_\omega \bar{\sigma}\left(H_{\tilde{z}\tilde{w}}(j\omega)\right)$$

The above criterion provides a single number based on the overall transfer function frequency response, $H_{\tilde{z}\tilde{w}}(j\omega)$, to optimize against. Software to compute the maximum singular value and the ∞-norm is available in many mathematical analysis packages, including Matlab and Xmath.

4.2 The μ Small-Gain Robustness Criterion

Any practical control design must be resilient in the face of uncertainty in its operating environment. Physical reasons for system uncertainty include component tolerances and degradation due to aging. These tolerances give rise to vehicle-to-vehicle variations that must be addressed when designing a single controller for a fleet of vehicles. Uncertainty must also be accounted for when using model-based robust control design approaches, due to the fact that even in the best conditions, the plant model used in the optimization is not perfect. It is thus necessary to account for *unmodeled dynamics*, which are typically small at low frequencies and increase at higher frequencies. In fact, it is this latter aspect of uncertainty that is the focus of the current work, since the goal is to design a controller for a one-of-a-kind demonstration vehicle. The purpose of this section is to establish precisely the properties that the closed loop system must have to ensure stability in the presence of uncertainty.

Recall from Section 3 that perturbations are inserted into the model to address robustness issues. In this work, robustness is quantified via a key result known as the *small-gain* theorem. In its simplest form, the small gain theorem states that for all *single* perturbations, $\delta_i \in \mathbb{C}$, satisfying the magnitude condition $|\delta_i| < 1$ (see Figure 7), the system will remain stable if the following ∞-norm condition holds:

$$\|w_{q_i} H_{q_i p_i}\|_\infty < 1 \tag{6}$$

Alternatively, in terms of a design requirement, since $H_{q_i p_i}$ is a function of the controller, K should be chosen such that

$$|H_{q_i p_i}(j\omega)| < \frac{1}{|w_{q_i}(j\omega)|}, \forall \omega \tag{7}$$

It is seen from (7) that the inverse of the perturbation magnitude serves as an upper bound on the frequency response magnitude function, $|H_{q_i p_i}(j\omega)|$. Therefore, by examining the four bode

magnitude plots $\left|H_{q_i p_i}(j\omega)\right|, i = 1...4$, designs can be compared with respect to the relative robustness of each controller path. These four plots will serve as the primary means of arriving at the robustness weightings in the design problem; the details are given in Section 5.2.

Note that the above analysis provides a *loop-by-loop* stability analysis. This is analogous to determining classical gain and phase margins by "breaking the loop" at the actuator and feedback sensors, one at a time. In order to evaluate and design for robust stability in the presence of all perturbations appearing simultaneously, further analysis is needed. To this end, consider Figure 9(A), which explicitly shows the normalized perturbation structure introduced in Section 3.3 (see Figure 7) in the standard framework. The scope of the robust stability problem is also shown via the dashed box (i.e. w and z are not considered).

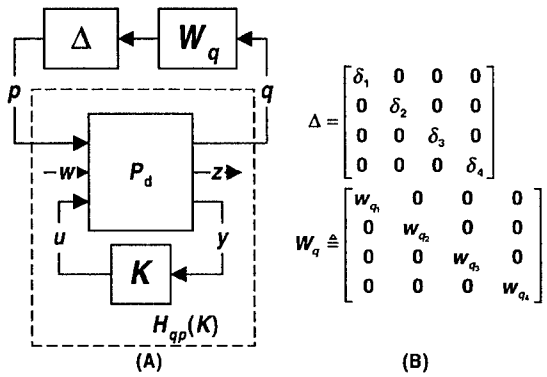

FIGURE 9: (A) NORMALIZED PERTURBATION STRUCTURE (B) DETAILS OF Δ AND W_q

The matrix W_q combines the individual perturbation weights, w_{q_i}, in a diagonal matrix corresponding to the diagonal structure of Δ. These matrices are shown in Figure 9(B). The diagonal matrix structure captures the decoupled nature of the perturbation model, i.e., perturbation δ_i only influences the i^{th} channel

The goal is now to obtain a condition on the matrix transfer function $H_{qp}(K)$ that guarantees stability in the presence of all four perturbations. A direct generalization of the single perturbation condition (6) is the small-gain condition

$$\left\| W_q H_{qp} \right\|_\infty < 1 \tag{8}$$

This stability result does indeed address the case of multiple perturbations, however, the perturbation matrix in this formulation is assumed to have a *full* structure, as opposed to the diagonal structure of Figure 9. Therefore, any stability assessment made using (8) will be unnecessarily conservative. Imposing such a condition on the design will result in severely compromised performance. Because of this issue, it is desirable to have a stability measure which takes into account the diagonal structure of the perturbation matrix.

To address the issue of conservatism when dealing with a system perturbation matrix having an inherent diagonal structure, the concept of μ was developed. Only a basic result from the theory of μ that is relevant to the current problem will be presented here. For more complete details, see [4] and the references therein. The result needed generalizes the small gain condition (8) to accommodate the fact that the perturbation has a diagonal structure, as follows:

$$\left\|W_q H_{qp}\right\|_\mu \triangleq \max_\omega \mu\left(W_q(j\omega)H_{qp}(j\omega)\right) < 1$$

where the function μ is a generalization of the maximum singular value, and is taken with respect to the specific diagonal structure of Δ. Thus μ provides a new notion of matrix size that applies specifically to a complex matrix (e.g. a frequency response matrix) connected in a feedback configuration to a block diagonal matrix. Maximizing μ over frequency provides the desired measure of *system* size, and provides a non-conservative stability criterion for systems with multiple complex uncertainties.

4.3 Combined Performance and Robustness Design Framework

The development of the previous two subsections is summarized in the block diagram of Figure 10.

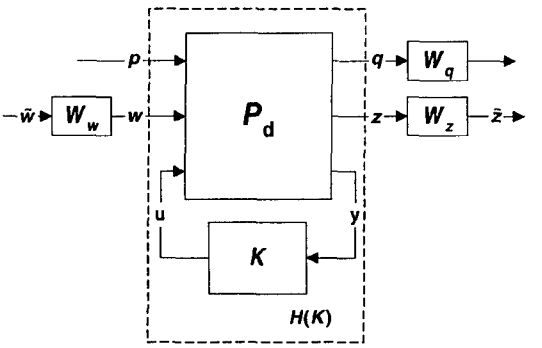

FIGURE 10: SUMMARY OF ROBUST PERFORMANCE DESIGN FRAMEWORK

In this view, all weighting functions are explicitly shown. These parameters represent the designer's "tuning knobs," which allow various control design tradeoffs to be explored. Both performance and robustness objectives introduced in the previous subsections can be combined into a single framework using μ. This is known as the "robust performance" problem, and is obtained by first combining the performance and robustness inputs and outputs:

$$w_{\text{rp}} = \begin{bmatrix} p \\ w \end{bmatrix}, \quad z_{\text{rp}} = \begin{bmatrix} q \\ z \end{bmatrix}$$

The corresponding combined input and output weights are:

$$W_{w_{\text{rp}}} = \begin{bmatrix} I_p & 0 \\ 0 & W_w \end{bmatrix}, \quad W_{z_{\text{rp}}} = \begin{bmatrix} W_q & 0 \\ 0 & W_z \end{bmatrix}$$

where I_p is a $p \times p$ identity matrix. The combined robust performance criteria is:

$$\left\|W_{z_{\text{rp}}} H W_{w_{\text{rp}}}\right\|_\mu < 1 \tag{9}$$

with μ taken with respect to the following augmented uncertainty structure:

$$\Delta_{rp} = \begin{bmatrix} \Delta_{rs} & 0 \\ 0 & \Delta_{perf} \end{bmatrix}$$

where Δ_{rs} is the diagonal uncertainty structure of Section 4.2, and Δ_{perf} is a complex valued matrix having as many rows as elements in w, and as many columns as elements in z.

5 DESIGN RESULTS

The Matlab Mu Analysis and Synthesis Toolbox provides routines to design a controller based on an iterative reduction of the left side of (9). The output of this design algorithm is a *state-space system*, i.e. a system defined by the following equations:

$$\dot{x} = Ax + By$$
$$u = Cx + Dy$$

where x is the state vector, $\dot{x}$ is the time derivative of the state vector, y is the sensor vector, and u is the controller output. The variables A, B, C, and D are appropriately dimensioned matrix parameters that define the controller. The computational complexity of the controller is determined by the size, or *order*, of the state vector, x. Larger state vectors require more computation from the processor. Note the square matrix A dominates the computational burden; since the number of elements in this matrix increase in a manner proportional to the *square* of the number of states. A property of the μ-synthesis design algorithm is that it produces controllers having the same number of states as the design plant, which is the number of states of the plant dynamics plus the number of states in all the design weighting parameters. Because of this, model reduction techniques are commonly applied, which can decrease the number of states quite dramatically. Following this reduction, the controller is converted into a discrete-time system for implementation on the target hardware. This yields a controller of the form:

$$x_{k+1} = A_T x_k + B_T y_k$$
$$u_k = C_T x_k + D_T y_k$$

where k is an integer sample index assuming a sampling time of T, and A_T, B_T, C_T, and D_T are the controller matrices which are implemented in the vehicle processor.

As described in the previous section, a robust control design in the current framework is equivalent to specifying the design weighting parameters W_z, W_w, and W_q. Sections 5.1 and 5.2 describe the choices made for these design parameters. Section 5.3 compares the bump course stabilization performance of the μ-synthesis controller with a classically tuned controller.

5.1 Performance Design Weights

Recall that defining performance is equivalent to defining the weighting matrices, W_w and W_z, defined in (4). Consider first the disturbance component, W_d. Its friction term, w_{T_f}, is chosen as the typical trunnion friction level for an M1A2 vehicle. The terrain disturbance terms, $w_{\dot{\theta}_T}$ and $\ddot{y}_T$, are chosen as the typical rms statistics for a bump course run. It was found that the

design is not particularly sensitive to the choices of these scaling parameters; their main function is to establish general order-of-magnitude differences in the signal values.

The second component of W_w, W_n, represents the approximate contribution of sensor noise to the feedback and feedforward signals. This can be viewed as a specification that the control design should not amplify sensor noise, which can arise from the finite resolution of the sensor, as well as the noise floor of the electronic hardware. This set of parameters can thus be interpreted as containing information regarding the accuracy of each sensor. For the M1A2 system, these parameters are chosen as follows:

$$W_n = \left[\begin{array}{c|c} W_{\text{fb}} & 0 \\ \hline 0 & W_{\text{ff}} \end{array}\right] = \left[\begin{array}{ccc|cc} \dfrac{10\times10^{-6}s}{s+2\pi(100)} & 0 & 0 & & \\ 0 & 10^{-3} & 0 & \multicolumn{2}{c}{0} \\ 0 & 0 & 10 & & \\ \hline \multicolumn{3}{c|}{} & 10^{-3} & 0 \\ \multicolumn{3}{c|}{0} & 0 & 0.02 \end{array}\right]$$

Note that for the resolver feedback of the trunnion position error, it must be assumed that there is no dc noise component (i.e. a position offset) because it would be impossible to reject, due to the fact that positional information is not contained in any other sensor. A first order high-pass filter is therefore used to eliminate such a noise component from consideration.

The performance output weighting matrix, W_z, is now chosen. The weighting functions in W_z provide the means of specifying the performance objectives of the control design. This is in contrast to the input weight W_n, which is used simply to establish general signal magnitudes. A natural starting point for obtaining the muzzle error weighting, w_e, is via the M1A2 rejection ratio specification, $R(\omega)$, which is a stabilization performance bound defined as follows:

$$\frac{\text{PSD}(\phi_t)}{\text{PSD}(\dot{\theta}_T)} < R(\omega)$$

In the context of the design framework of Figure 10, the rejection ratio can be interpreted as a bound on the magnitude of H_{ed} as follows:

$$\left|H_{ed}(j\omega)\right| < R(\omega), \forall\omega$$

This expression can alternatively be stated in the form of a robust control performance specification as follows:

$$\max_{\omega}\left[R^{-1}(\omega)H_{ed}(j\omega)\right] = \left\|R^{-1}H_{ed}\right\|_{\infty} < 1 \qquad (10)$$

Therefore, $R^{-1}(\omega)$ can serve as a starting point for determining the performance weight, w_e. Since the rejection ratio specification is conservative from a design standpoint, iterations on w_e are necessary to further refine the performance specification. Specifying higher levels of performance (i.e. smaller muzzle error) requires a larger performance weight, i.e.

$$w_e(j\omega) > R^{-1}(\omega)$$

The final choice for w_e was arrived at via trial-and-error design iterations, and is depicted via a plot of the product $w_e(j\omega)R(\omega)$, shown in Figure 11.

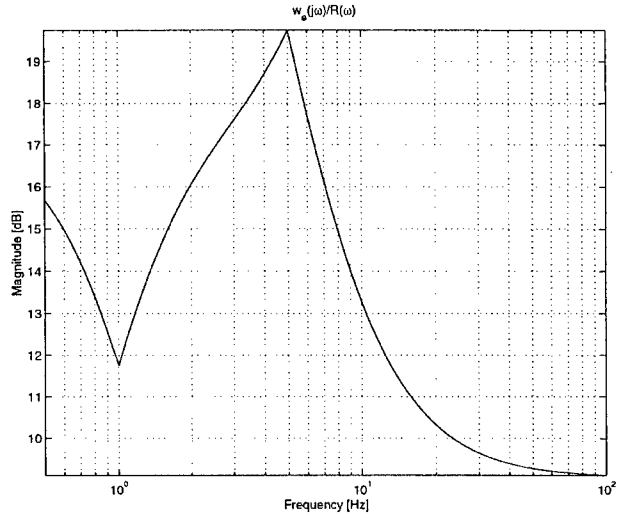

FIGURE 11: NORMALIZED PERFORMANCE SPECIFICATION PLOT

A normalized view of the performance specification is necessary due to the sensitivity of the underlying M1A2 performance requirement. In this plot, 0 dB indicates the performance specification is exactly consistent with the rejection ratio. Larger values represent a more stringent specification.

Finally, the actuator weight, w_u is chosen. This specification is an upper bound on the actuator authority used by the controller, and must be chosen based on the capabilities of the physical system. It is typically chosen so that the controller uses as much of the usable actuator authority as possible, to maximize performance. Furthermore, it should ensure that the controller commands *roll-off* at high frequencies. For the current M1A2 system, this parameter was chosen to be:

$$w_u = 0.56\left[\frac{s/\omega_1 + 1}{s/\omega_2 + 1}\right]^5, \qquad \omega_1 = 2\pi(200), \omega_2 = 2\pi(10^4)$$

Note w_u is a lead-lag filter that ramps up at 200Hz to enforce a roll-off property. The 10 kHz leveling off is due to a technical requirement of the optimization software that all weighting functions be proper.

5.2 Robustness Design Weights

In any control design problem, a fundamental tradeoff exists between performance and robustness. Therefore, a key design goal is to provide the *minimum* robustness required by the system in order to *maximize* system performance. Recall that in the current setting, robustness is addressed via the frequency-dependent weighting parameters, w_{q_i}, which focus the μ-synthesis

optimization on robustness to the i^{th} multiplicative uncertainty. Since an uncertainty is, by definition, not well known, these parameters must be chosen carefully. Ultimate determination of robustness parameters must be made in conjunction with vehicle testing. The purpose of this section is to establish the method used here to guide the selection of the robustness weights.

In addition to their interpretation as a frequency-dependent characterization of the uncertainty magnitude, the robustness weights can alternatively be viewed as frequency-dependent "design knobs" – larger magnitudes increase optimization focus on the robustness objective. Typically this involves trading off performance in that frequency range. As described in Section 4.2, the robustness of the individual feedback loops can be evaluated via the four plots, $\left|H_{q_i p_i}(j\omega)\right|, i=1\ldots4$. Using these plots, the following iterative procedure was used to arrive at the robustness weights:

1) Start with $w_{q_i}=0, i=1\ldots4$.
2) Perform μ-synthesis to generate a controller
3) Compare the resulting closed loop properties to that of a "reference" system, H_{ref}
   a) Plot the robustness plots $\left|H_{q_i p_i}(j\omega)\right|, i=1\ldots4$, for both control systems
   b) Plot the performance plot $\bar{\sigma}\left[W_z(j\omega)H_{zw}(j\omega)W_w(j\omega)\right]$ for both control systems
4) If the plots from 3a and 3b are desirable, then proceed to simulation and implementation; else introduce/modify w_{q_i} according to the general guidelines of Section 4.2
5) If the implementation exhibits problems such as instability or resonance, introduce/modify w_{q_i} as necessary according to the general guidelines of Section 4.2

For this project, the controller used as H_{ref} varied throughout the study. Initially, it was the nominal M1A2 closed loop system, since it is known to have good performance and robustness properties. Once hardware was available, H_{ref} was the most recent controller iteration. Bode magnitude plots for $w_{q_i}, i=1\ldots3$, are shown in Figure 12, while $w_{q_4}=0$. The frequency dependence of the weighting functions has been utilized to tailor robustness around problem frequencies in the system.

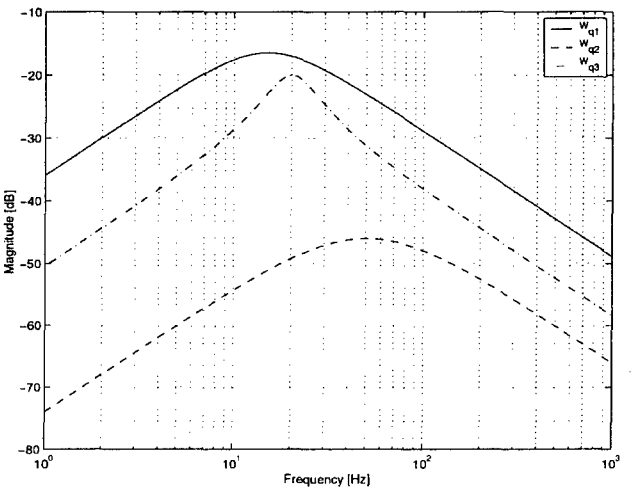

FIGURE 12: ROBUSTNESS DESIGN WEIGHTS

5.3 Bump Course Test Results

Application of the μ-synthesis design routines yielded a 47^{th} order continuous time controller. Subsequent model reduction and discretization resulted in a 22^{nd} order digital controller implemented on the M1A2 system. The stabilization testing shown here was carried out at Aberdeen Proving Grounds, using RRC-9 bumps with a vehicle speed of 10 mph. To evaluate the performance properties of the robust control design and gain the most insight possible, a classically tuned stabilization design was also developed for the long gun system. The details of the classical design will not be given; however, the fundamental difference in philosophy between the two approaches is simply described. Namely, the performance objective of the classical control design is to maintain small trunnion-pointing error, as measured by the gun-trunnion resolver, whereas the performance objective of the robust control design is to maintain small *muzzle*-pointing error. The model-based nature of the robust control design makes it possible to optimize the design goal about a quantity that is not sensed. The key comparison is shown in Table 1, where the terrain disturbance and gun response RMS statistics are compared for each controller.

TABLE 1: ROBUST CONTROLLER BUMP COURSE RMS STATISTICS (RELATIVE TO CLASSICAL DESIGN)

	TERRAIN DISTURBANCE		GUN RESPONSE	
	FF_ACCEL ($\ddot{y}_T$)	FF_GYRO ($\dot{\theta}_T$)	TRUN ERROR (ϕ_t)	MUZZLE ERROR (ϕ_m)
$\Delta\%$	13	9.6	94	-8.1

To convincingly illustrate the muzzle performance of the robust controller, bump course runs were chosen where the terrain disturbances are larger for the robust controller. The most striking difference in the gun response statistics is in the trunnion response. Namely, Table 1 shows that, relative to the classical controller, the robust controller achieves an 8.1% reduction in the muzzle error with a 94% *increase* in the trunnion error. This behavior is somewhat counterintuitive, however, it is consistent with the robust control problem formulation since the performance variable in the μ-synthesis optimization contained the muzzle angle and not the trunnion angle.

Additional insight is obtained by comparing the power spectral densities (PSD's) of the above signals, shown in Figure 13. The small trunnion error of the classical controller is evident across all frequencies. The muzzle behavior, however, is interesting in that the classical controller response exhibits peaking at 10 Hz. The modern controller does not excite this frequency at all. In fact, analysis has shown that muzzle vibration can be excited as a result of a high bandwidth trunnion loop, such as that in the classical controller [5]. Therefore, the robust control design has provided a means of obtaining small muzzle errors without a high bandwidth trunnion loop; such a solution would not have been found using conventional design techniques.

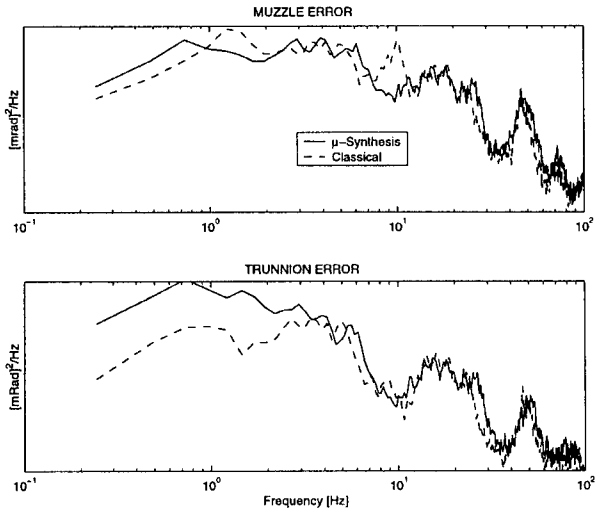

FIGURE 13: POWER SPECTRAL DENSITIES OF GUN RESPONSE

6 CONCLUSIONS

This work has demonstrated the feasibility of using a model-based optimal control design methodology for gun stabilization. This approach is characterized by specifying desired closed-loop performance and robustness objectives. This is an attractive design paradigm, focusing on the higher level issue of *what to do*, instead of *how to do it*. The latter issue is addressed in an automated fashion via the optimization process. However, selection of the frequency weighting parameters is, in general, non-trivial, and must be done with care. Specifically, since the performance and robustness objectives relate to desired closed loop performance, it is possible to specify levels of performance and robustness that are not simultaneously achievable by the system. In such a case, either the design optimization algorithm will not converge, or the resulting design simply will not meet the objectives. Thus the design difficulty lies in gaining experience in understanding how best to translate the physical design objectives into the performance and robustness weighting parameters. This has been achieved here using a combination of simulations and vehicle testing. Once the general principals are established, more design work can be done via computer simulation, which greatly reduces development and testing expense.

REFERENCES

1. V. R. Marcopoli, Independent Research and Development Report, General Dynamics Proprietary Information, 1999.
2. D. J. Purdy, "Comparison of Balanced and Out Of Balance Main Battle Tank Armaments," Proceedings 9th U.S. Army Gun Dynamics Symposium, 1999.
3. S. Boyd and C. Barratt, *Linear Control Design – Limits of Performance*, Prentice-Hall, 1991.
4. G. Balas, J. C. Doyle, K. Glover, A. Packard, R. Smith, *μ-Analysis and Synthesis Toolbox*, The Mathworks, 1995.
5. J. Freudenberg, Independent Research and Development Report, General Dynamics Proprietary Information, 1999.